JOURNAL OF GUIDANCE, CONTROL, AND DYNAMICS
Vol. 21, No. 3, May–June 1998

Active Vibration Suppression in Flexible Spacecraft Attitude Tracking

S. Di Gennaro*
Università di L'Aquila, 67040 L'Aquila, Italy

The active suppression of vibrations of spacecraft flexible appendages during attitude tracking or large-angle maneuvers is discussed. On the basis of a model obtained using the Lagrangian approach and the unitary quaternion parameterization, piezoelectric actuators are used to damp the vibration of flexible booms induced during the maneuvers. The results of simulation reveal the interest and the practical feasibility of such a control scheme. The control law requires only the measure of the attitude and the angular velocity. The absence of flexible displacement and velocity sensors is compensated for by the presence of appropriate dynamics in the controller.

I. Introduction

THE active compensation of flexible bending during attitude maneuvers is an intriguing problem that has recently stimulated research activities. Both small satellites with flexible booms and antennas and large space stations composed of light deformable structures will get benefits from the development of distributed damping control. Moreover, due to the intensive use of deformable frames in the design of spatial stations, where weight and cost of structures are crucial issues, this is an important problem in future space missions, where pointing precision, shape control, and integrity of the structures are prior mission requirements.

For these large structures the dynamic behavior can be difficult to predict analytically. The main problems arise from the unreliability or impracticality of structural tests on Earth. The performance of controls designed on the basis of perfect model knowledge can be deteriorated, and these difficulties can lead to on-orbit behaviors, which can be substantially different from preflight ground test measures or analytic predictions. One way to overcome these problems could be the use of adaptive control schemes,[18–20] where the structural parameters are adapted during the space operation. An alternative to this approach is the use of structures with distributed actuators, sensors, and decentralized computation capabilities. This structure design makes them, in some sense, more intelligent and at the same time allows for the implementation of different control strategies, such as decentralized or hierarchical ones.

Among the active control schemes presently available, those based on distributed piezoelectric actuators and sensors have been the subject of renewed interest in the field of smart structures and structural vibration control. In fact, these devices turn out to be experimentally effective in damping out the vibrations of simple structures. This characteristic, together with their intrinsic distributed nature, high displacement resolution, and wideband characteristics, i.e., lightness, high performance, and low power consumption, make these devices appealing candidates for controlling the vibration of structures with more complicated geometries. The research aim is, therefore, to exploit their integrability into structures with embedded or bounded piezoelectric layers.

There are many contributions on this subject in the literature. Most of them have the aim of determining an accurate modeling of structures with such piezoelectric actuators. Analytic models, experimentally tested, can be found in Refs. 21 and 22, whereas optimal control policies have been studied in Ref. 23 (also see references therein). The study carried out in Ref. 24 underlines the advantages of a control making use of piezoelectric actuators. With the present technology, these actuators can be more effective for damping vibrations of small amplitude. Nevertheless, the fine tuning of the attitude of a spacecraft structure is of crucial importance, especially at the very beginning and at the end of a large rapid maneuver or during the tracking of a desired trajectory. In fact, these actuators have been revealed to be very effective for suppressing the vibrations of flexible appendages, as shown in Refs. 25 and 26, where these actuators have been tested on experimental structures. Other motivations and benefits in the use of active control technology can be found in Ref. 27.

Far from giving a complete response to all of the open problems that are involved in active vibration control, in this work we propose a solution for attitude control of a spacecraft with flexible elements, following a Lyapunov approach. This controller consists of a dynamic compensation that uses only attitude and angular velocity measures. Such a characteristic eliminates the need for measuring the whole state of the system and, in particular, modal displacements and velocities. The independence of the controller on real-time measures of flexibility must not be considered a defective characteristic. As a matter of fact, our compensator, composed of a dynamic part that, roughly speaking, represents an internal model of the flexible dynamics develops a control action based on the difference between the measured and estimated effects on the controlled variables.

The spacecraft is supposed to constitute a rigid main body and a flexible boom carrying a payload. The piezoelectric actuators are here used to actively dump the negative effects of vibrations induced by maneuvers, which could destabilize the spacecraft behavior in presence of saturation on inputs. The problems encountered are the tracking of a desired trajectory and the execution of large attitude maneuvers. It has been shown that the first turns out to be an attitude maneuver problem of a time-varying system, the time-varying term depending on the desired trajectory. Hence, the kinematics are described in terms of error quaternions of the actual attitude with respect to a desired one. The actuators used are gas jets and/or reaction wheels, together with piezoelectric films bounded to the flexible boom. Their expansion or contraction, due to the applied electric field aligned or opposed with the film polarization axis, determines longitudinal bending stresses used to counteract the boom's undesirable vibrations.

In the following section, the kinematic equations of the attitude error and the dynamics of the spacecraft are recalled on the basis of the Lagrangian approach. In Sec. III, the Lyapunov technique is used for designing a dynamic controller based on position and angular velocity measures. Different control schemes are considered, either in case of gas jet or reaction wheel control mode. Simulations in Sec. IV illustrate the performances of the proposed controller. These can also be considered as a robustness test because the controller is applied to a more accurate spacecraft model. A discussion of the presented results concludes the paper.

Received April 25, 1997; revision received Oct. 6, 1997; accepted for publication Oct. 9, 1997.

*Assistant Professor, Dipartimento di Ingegneria Elettrica, Poggio di Roio. E-mail: digennar@riscdis.ing.uniroma1.it.

II. Mathematical Model of a Flexible Spacecraft

The kinematic equations will be given in terms of unitary quaternions $e_0(t), e_1(t), e_2(t), e_3(t)$ (Refs. 3, 28, and 29). They express the

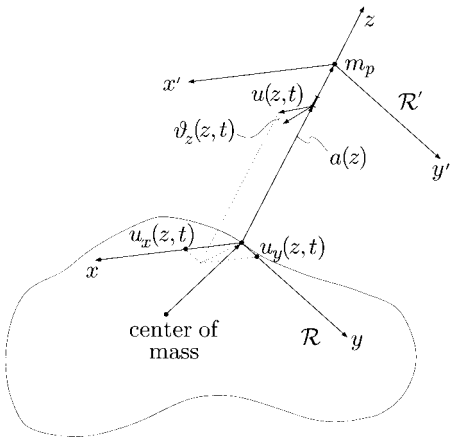

Fig. 1 Spacecraft with flexible booms.

attitude error of the reference $\mathcal{R}$ fixed with the main body, having its origin in the attachment point of the flexible boom with the main body (see Fig. 1), with respect to a desired reference frame $\mathcal{R}_d$. Their dynamics are

$$\begin{bmatrix} \dot{e}_0(t) \\ \dot{\boldsymbol{e}}(t) \end{bmatrix} = \frac{1}{2} \begin{bmatrix} -\boldsymbol{e}^T(t) \\ R(t) \end{bmatrix} [\boldsymbol{\omega}(t) - \boldsymbol{\omega}_d(t)] \tag{1}$$

where

$$\boldsymbol{e}(t) = \begin{bmatrix} e_1(t) \\ e_2(t) \\ e_3(t) \end{bmatrix}$$

$\omega(t)$ and $\omega_d(t)$ are the angular velocities of $\mathcal{R}$ and $\mathcal{R}_d$, and

$$R(t) = \begin{bmatrix} e_0(t) & -e_3(t) & e_2(t) \\ e_3(t) & e_0(t) & -e_1(t) \\ -e_2(t) & e_1(t) & e_0(t) \end{bmatrix} = e_0(t)I + \tilde{\boldsymbol{e}}(t)$$

$$\tilde{\boldsymbol{e}} = \begin{bmatrix} 0 & -e_3(t) & e_2(t) \\ e_3(t) & 0 & -e_1(t) \\ -e_2(t) & e_1(t) & 0 \end{bmatrix}$$

Note that the quaternions are subject to the constraint condition

$$\sum_{i=0}^{3} e_i^2(t) = 1$$

so that $e_0(t)$ can be computed from the components of the $\boldsymbol{e}(t)$ vector.

The dynamic equations can be derived by the Lagrangian approach.[30,31] In the following we refer to Refs. 1, 2, and 8 for details of the derivation of spacecraft dynamics. The elastic deformations of the mass element of coordinate z of the flexible appendage along the x and y axes are $u_x(z,t)$ and $u_y(z,t)$, whereas the torsional deformation around the z axis is $\vartheta_z(z,t)$. They can be approximated as a linear combination of a finite number of admissible functions Φ_{xi}, Φ_{yi}, and Φ_{zi},

$$u_x(z,t) = \sum_{i=1}^{N} \Phi_{xi}(z)\eta_i(t) = \boldsymbol{\Phi}_x^T(z)\boldsymbol{\eta}(t)$$

$$u_y(z,t) = \sum_{i=1}^{N} \Phi_{yi}(z)\eta_i(t) = \boldsymbol{\Phi}_y^T(z)\boldsymbol{\eta}(t)$$

$$\vartheta_z(z,t) = \sum_{i=1}^{N} \Phi_{zi}(z)\eta_i(t) = \boldsymbol{\Phi}_z^T(z)\boldsymbol{\eta}(t)$$

Here $\eta_i(t)$, $i = 1, \ldots, N$, are the modal deformation coordinates and N is the number of significant modes. Obviously, $\boldsymbol{\eta}(t) = [\eta_1(t) \ \cdots \ \eta_N(t)]^T$.

The rotational and elastic dynamics of the spacecraft are obtained by computing the kinetic and potential energies and then applying the Lagrange equations.[8] The total kinetic energy $T(t)$ of the flexible spacecraft is the sum of the kinetic energies associated with the main body, the flexible boom, and the object placed on the tip of the boom. The potential energy is due to the flexibility of the boom, whereas the effect of the (nonconservative) viscous damping forces can be taken into account by supposing that they are proportional to the generalized velocities and are taken into account by introducing a Rayleigh dissipation function. Finally, the boom is covered with two piezoelectric layers reacting to the x- and y-direction deformations. These layers are homogeneous, isotropic, perfectly bonded to the boom, and of constant thickness. If $u_{px}(t)$ and $u_{py}(t)$ are the voltages applied to the films, the bending moments around the neutral axis of the composite boom are given by $M_y(t) = -c_{px}u_{px}(t)$ and $M_x(t) = -c_{py}u_{py}(t)$, with c_{px} and c_{py} constants depending on the geometry and the nature of materials.[23–25] Here it is supposed that each film is not seriously influenced by the flection induced by the other.

By considering small displacements, from the Lagrange equations one obtains[10,11]

$$\begin{aligned} &J_0\dot{\boldsymbol{\omega}}(t) + J_r\dot{\boldsymbol{\Omega}}(t) + \delta_0^T\ddot{\boldsymbol{\eta}}(t) \\ &\quad = -\tilde{\boldsymbol{\omega}}\left[J_0\boldsymbol{\omega}(t) + J_r\boldsymbol{\Omega}(t) + \delta_0^T\dot{\boldsymbol{\eta}}(t)\right] + \boldsymbol{u}_g(t) \\ &\qquad J_r[\dot{\boldsymbol{\omega}}(t) + \dot{\boldsymbol{\Omega}}(t)] = \boldsymbol{u}_r(t) \\ &\ddot{\boldsymbol{\eta}}(t) + C\dot{\boldsymbol{\eta}}(t) + K\boldsymbol{\eta}(t) = -\delta_0\dot{\boldsymbol{\omega}}(t) - \delta_2\boldsymbol{u}_p(t) \end{aligned} \tag{2}$$

Note that with the small displacement approximation a simple model is derived; this is easy to manipulate and more suitable for control design. The exact model, time varying and more difficult to handle, can be used instead for verifying the effectiveness of the control law, derived on the basis of the simplified model. Another difference between these two models is the number of elastic modes considered. In Eq. (2) J_0 is the total symmetric inertia matrix of the undeformed structure, J_r is the symmetric inertia matrix of the reaction wheels, and $\boldsymbol{\omega}(t)$ and $\boldsymbol{\Omega}(t)$ are the angular velocities of the main body and of the reaction wheels. Furthermore, δ_0 is the coupling matrix between flexible and rigid dynamics, and δ_2 is the coupling matrix between the piezoelectric actuators and the flexible dynamics. Moreover, $\boldsymbol{u}_g$ is the torque acting on the main body and produced by the gas jets, $\boldsymbol{u}_r(t)$ is the torque imposed by the reaction wheels, and

$$\boldsymbol{u}_p(t) = \begin{bmatrix} u_{px}(t) \\ u_{py}(t) \end{bmatrix}$$

is the vector of the voltages applied to the piezoelectric layers. Finally, $C = \text{diag}\{2\zeta_1\omega_1, \ldots, 2\zeta_N\omega_N\}$ and $K = \text{diag}\{\omega_1^2, \ldots, \omega_N^2\}$ are the damping and stiffness matrices, respectively.

The state variables chosen to describe the dynamics of the spacecraft are the quaternions $e_0(t)$ and $\boldsymbol{e}(t)$, the spacecraft error angular velocity $\boldsymbol{\omega}_e(t) = \boldsymbol{\omega}(t) - \boldsymbol{\omega}_d(t)$, the reaction wheels angular velocity $\boldsymbol{\Omega}(t)$, the modal displacements $\boldsymbol{\eta}(t)$ relative to the main body, and the variable

$$\boldsymbol{\psi}(t) = \delta_0\boldsymbol{\omega}_e(t) + \dot{\boldsymbol{\eta}}(t) \tag{3}$$

representing the difference between the total modal velocity $\delta_0\boldsymbol{\omega}(t) + \dot{\boldsymbol{\eta}}(t)$ and $\boldsymbol{\omega}_d(t)$ expressed in modal coordinates. Further on this will simplify the computational developments in the next sections, maintaining a physical meaning of the state variables. Hence, we obtain

$$\begin{aligned} &\dot{e}_0(t) = -\tfrac{1}{2}\boldsymbol{e}^T(t)\boldsymbol{\omega}_e(t), \qquad \dot{\boldsymbol{e}}(t) = \tfrac{1}{2}R(t)\boldsymbol{\omega}_e(t) \\ &\dot{\boldsymbol{\omega}}_e(t) = J_{10}^{-1}\Big\{-N[\boldsymbol{\omega}_e(t), \boldsymbol{\Omega}(t), \boldsymbol{\psi}(t), \boldsymbol{\omega}_d(t)] \\ &\quad + \delta_0^T[C\boldsymbol{\psi}(t) + K\boldsymbol{\eta}(t)] - \delta_0^T C\delta_0\boldsymbol{\omega}_e(t) \\ &\quad + \boldsymbol{u}_g(t) - \boldsymbol{u}_r(t) + \Delta_0\boldsymbol{u}_p(t)\Big\} - \dot{\boldsymbol{\omega}}_d(t) \\ &\dot{\boldsymbol{\Omega}}(t) = -\dot{\boldsymbol{\omega}}_e(t) + J_r^{-1}\boldsymbol{u}_r(t) - \dot{\boldsymbol{\omega}}_d(t), \qquad \dot{\boldsymbol{\eta}}(t) = \boldsymbol{\psi}(t) - \delta_0\boldsymbol{\omega}_e(t) \\ &\dot{\boldsymbol{\psi}}(t) = -[C\boldsymbol{\psi}(t) + K\boldsymbol{\eta}(t)] + C\delta_0\boldsymbol{\omega}_e(t) - \delta_2\boldsymbol{u}_p(t) - \delta_0\dot{\boldsymbol{\omega}}_d(t) \end{aligned} \tag{4}$$

with

$$J_{10} = J_0 - J_r - \delta_0^T \delta_0 \tag{5}$$

$$\boldsymbol{N}[\boldsymbol{\omega}_e(t), \boldsymbol{\Omega}(t), \boldsymbol{\psi}(t), \boldsymbol{\omega}_d(t)] = [\tilde{\boldsymbol{\omega}}_e(t) + \tilde{\boldsymbol{\omega}}_d(t)] \times \left[\left(J_0 - \delta_0^T \delta_0\right)\boldsymbol{\omega}_e(t) + J_r \boldsymbol{\Omega}(t) + \delta_0^T \boldsymbol{\psi}(t) + J_0 \boldsymbol{\omega}_d(t)\right] \tag{6}$$

and $\Delta_0 = \delta_0^T \delta_2$. This model will be used in the following section to derive the desired control laws.

Note that model (4) is similar to that used in Refs. 10 and 11, and the main differences are due to the term of the piezoelectric actuators and the different choice of state variables.

Remark 1. If the reaction wheels are absent, the corresponding dynamics must be removed. This leads to the elimination of the dynamics of the variable $\boldsymbol{\Omega}(t)$ in the model and to the setting of $\boldsymbol{u}_r(t)$ and J_r to zero in the expressions of J_{10} and of the gyroscopic term $\boldsymbol{N}$:

$$J_{10} = J_0 - \delta_0^T \delta_0 \tag{7}$$

$$\begin{aligned} \boldsymbol{N} &= [\tilde{\boldsymbol{\omega}}_e(t) + \tilde{\boldsymbol{\omega}}_d(t)]\left[J_{10}\boldsymbol{\omega}_e(t) + \delta_0^T \boldsymbol{\psi}(t) + J_0 \boldsymbol{\omega}_d(t)\right] \\ &= \boldsymbol{N}[\boldsymbol{\omega}_e(t), \boldsymbol{\psi}(t), \boldsymbol{\omega}_d(t)] \end{aligned} \tag{8}$$

□

The outputs to be controlled are the quaternion vector $\boldsymbol{y}_1(t) = \boldsymbol{e}(t)$ and the physical displacement vector $\boldsymbol{y}_2(t) = \Phi^T(l)\boldsymbol{\eta}(t)$ of the flexible appendage tip. Here $\Phi(l)$ is a matrix that transforms the modal coordinates into real ones, calculated at the tip of the appendage of length l. The control must ensure the convergence to zero of both outputs as t tends to infinity, that is, it must allow the asymptotic tracking of the desired attitude with zero tip displacement.

III. Design of a Dynamic Controller with Position and Angular Velocity Measures

In this section we develop a controller for actively damping vibrations, on the basis of the simplified model (4). The role of the piezoelectric actuators is to increase the internal damping of the flexible structure. The main problems are caused by the difficulty in determining the modal variables. To overcome these problems and to reduce the number of sensors, a dynamic controller is proposed hereinafter, which makes use of spacecraft position and angular velocity measures. As already stated, the control aim is to ensure that the outputs tend asymptotically to zero. Nevertheless, all of the state variables representing errors implied by the tracking maneuver must tend to zero. The stability study of the state-space origin and the derivation of the controller solving the problem are conducted by making use of the Lyapunov function technique. Because the system is time varying, the asymptotic stability is deduced by using the Barbalat theorem.[32]

A. Gas Jets Control Mode

The first case concerns a spacecraft actuated only by gas jets. The reaction wheels are, therefore, absent. The estimates of modal variables are denoted by $\hat{\boldsymbol{\eta}}(t)$ and $\hat{\boldsymbol{\psi}}(t)$. We demonstrate that the dynamic controller that ensures the control objectives is that given in the following statement.

Theorem 1. Let us consider the dynamic controller

$$\begin{aligned} \begin{bmatrix} \dot{\hat{\boldsymbol{\eta}}}(t) \\ \dot{\hat{\boldsymbol{\psi}}}(t) \end{bmatrix} &= \boldsymbol{\Gamma}[\boldsymbol{\omega}(t), \hat{\boldsymbol{\eta}}(t), \hat{\boldsymbol{\psi}}(t), \boldsymbol{\omega}_d(t)] \\ &= \bar{A}_c \begin{bmatrix} \hat{\boldsymbol{\eta}}(t) \\ \hat{\boldsymbol{\psi}}(t) \end{bmatrix} - A_c B_c \delta_0 \boldsymbol{\omega}_e(t) - B_c \delta_0 \dot{\boldsymbol{\omega}}_d(t) \\ &\quad + P_2^{-1}\left(\left\{\begin{matrix} K\delta_0 \\ \delta_0[\tilde{\boldsymbol{\omega}}_e(t) + \tilde{\boldsymbol{\omega}}_d(t)] + C\delta_0 \end{matrix}\right\}[\boldsymbol{e}(t) + \boldsymbol{\omega}_e(t)] \right. \\ &\quad \left. + \begin{pmatrix} \lambda_1 I \\ \lambda_2 I \end{pmatrix} \delta_2 \delta_2^T B_c^T P_1 \begin{bmatrix} \hat{\boldsymbol{\eta}}(t) \\ \hat{\boldsymbol{\psi}}(t) \end{bmatrix}\right) \end{aligned} \tag{9}$$

$$\begin{aligned} \boldsymbol{u}_g(t) &= -k_p \boldsymbol{e}(t) - k_d \boldsymbol{\omega}_e(t) - \tfrac{1}{2} J_{10} R(t) \boldsymbol{\omega}_e(t) \\ &\quad + \boldsymbol{N}[\boldsymbol{\omega}_e(t), \hat{\boldsymbol{\psi}}(t), \boldsymbol{\omega}_d(t)] - \delta_0^T [C\hat{\boldsymbol{\psi}}(t) + K\hat{\boldsymbol{\eta}}(t)] \\ &\quad + \delta_0^T C \delta_0 \boldsymbol{\omega}_e(t) - \Delta_0 \boldsymbol{u}_{p1}(t) + J_{10}\dot{\boldsymbol{\omega}}_d(t) \end{aligned} \tag{10}$$

$$\boldsymbol{u}_p(t) = \boldsymbol{u}_{p1}(t) = \delta_2^T (\lambda_1 I \quad \lambda_2 I) \begin{bmatrix} \hat{\boldsymbol{\eta}}(t) \\ \hat{\boldsymbol{\psi}}(t) \end{bmatrix} \tag{11}$$

with J_{10} as in Eq. (7),

$$\begin{aligned} &\boldsymbol{N}[\boldsymbol{\omega}_e(t), \hat{\boldsymbol{\psi}}(t), \boldsymbol{\omega}_d(t)] \\ &\quad = [\tilde{\boldsymbol{\omega}}_e(t) + \tilde{\boldsymbol{\omega}}_d(t)][J_{10}\boldsymbol{\omega}_e(t) + \delta_0^T \hat{\boldsymbol{\psi}}(t) + J_0 \boldsymbol{\omega}_d(t)] \end{aligned}$$

and $k_p, k_d > 0$, $\lambda_1, \lambda_2 \geq 0$ fixed quantities,

$$A_c = \begin{pmatrix} 0 & I \\ -K & -C \end{pmatrix}, \qquad B_c = \begin{pmatrix} 0 \\ I \end{pmatrix}$$

$$\begin{aligned} \bar{A}_c &= A_c - B_c \delta_2 \delta_2^T (\lambda_1 I \quad \lambda_2 I) \\ &= \begin{bmatrix} 0 & I \\ -\left(K + \lambda_1 \delta_2 \delta_2^T\right) & -\left(C + \lambda_2 \delta_2 \delta_2^T\right) \end{bmatrix} \end{aligned}$$

and

$$P_i = P_i^T = \begin{pmatrix} P_{i1} & P_{i2} \\ P_{i2}^T & P_{i3} \end{pmatrix}, \qquad i = 1, 2$$

positive definite matrices, solutions of the equations

$$\frac{P_1 \bar{A}_c + \bar{A}_c^T P_1}{2} = -Q_1 < 0, \qquad \frac{P_2 A_c + A_c^T P_2}{2} = -Q_2 < 0 \tag{12}$$

where

$$\begin{aligned} Q_1 &= \begin{pmatrix} \lambda_\eta I & 0 \\ 0 & \lambda_\psi I \end{pmatrix} \\ Q_2 &= \begin{pmatrix} \lambda_{e_\eta} I & 0 \\ 0 & \lambda_{e_\psi} I \end{pmatrix} + \begin{pmatrix} \lambda_1 I \\ \lambda_2 I \end{pmatrix} \delta_2 \delta_2^T B_c^T P_1 \end{aligned} \tag{13}$$

are fixed positive-definite matrices, with $\lambda_\eta, \lambda_\psi, \lambda_{e_\eta}, \lambda_{e_\psi} > 0$. This solves the control problem for system (4) in the absence of reaction wheels, with a desired angular velocity $\omega_d(t) \in L_\infty[0, \infty)$ and derivative $\dot{\omega}_d(t) \in L_2[0, \infty) \cap L_\infty[0, \infty)$. □

Note that $Q_2 > 0$ for an appropriate choice of λ_{e_η} and λ_{e_ψ} and that the solutions P_i exist because $\sigma(\bar{A}_c) \subset \mathbb{C}^-$, $\sigma(A_c) \subset \mathbb{C}^-$, with $\sigma(\cdot)$ denoting the set of eigenvalues.

This result is proved by using the well-known Lyapunov function technique. Refer to Ref. 33 for further details. In this approach the stability nature of the origin of the state space, where the variables evolve, can be determined by examining the derivative of a (positive definite) Lyapunov function V along the trajectories of the system (4). The choice of V can be critical in some cases, whereas in others it is simply the energy of the system. Intuitively, if its variation along the system's trajectories is negative, the "system energy" decreases and the trajectories tend to the origin, which is asymptotically stable. When this derivative is less than or equal to zero, we can try to apply an extension of Lyapunov theory developed by La Salle. This again allows for the statement of the origin asymptotic stability. Unfortunately, the study is more complicated for time-varying systems; however, a very interesting tool that can be used in such cases is the Barbalat lemma. The starting point is again the choice of an appropriate Lyapunov function, which is here taken as a function composed of three contributions,

$$V_1[\boldsymbol{x}(t), t] = V_r[\boldsymbol{x}(t), t] + V_f[\boldsymbol{x}(t)] + V_d[\boldsymbol{x}(t)]$$

where

$$V_r[\boldsymbol{x}(t),t] = (k_p + k_d)\left\{[e_0(t)-1]^2 + \boldsymbol{e}^T(t)\boldsymbol{e}(t)\right\} + \tfrac{1}{2}[\boldsymbol{e}(t)+\boldsymbol{\omega}_e(t)]^T J_{10}[\boldsymbol{e}(t)+\boldsymbol{\omega}_e(t)] \tag{14}$$

$$V_f[\boldsymbol{x}(t)] = \frac{1}{2}[\boldsymbol{\eta}^T(t) \quad \boldsymbol{\psi}^T(t)]P_1\begin{bmatrix}\boldsymbol{\eta}(t)\\ \boldsymbol{\psi}(t)\end{bmatrix} \tag{15}$$

$$V_d[\boldsymbol{x}(t)] = \frac{1}{2}\begin{bmatrix}\boldsymbol{e}_\eta^T(t) & \boldsymbol{e}_\psi^T(t)\end{bmatrix}P_2\begin{bmatrix}\boldsymbol{e}_\eta(t)\\ \boldsymbol{e}_\psi(t)\end{bmatrix} \tag{16}$$

with $\boldsymbol{e}_\eta(t) = \boldsymbol{\eta}(t) - \hat{\boldsymbol{\eta}}(t)$, $\boldsymbol{e}_\psi(t) = \boldsymbol{\psi}(t) - \hat{\boldsymbol{\psi}}(t)$, and

$$\boldsymbol{x}(t) = \begin{bmatrix}\boldsymbol{e}^T(t) & \boldsymbol{\omega}_e^T(t) & \boldsymbol{\eta}^T(t) & \boldsymbol{\psi}^T(t) & \boldsymbol{e}_\eta^T(t) & \boldsymbol{e}_\psi^T(t)\end{bmatrix}^T$$

the vector of state variables. Remember that $e_0(t)$ is a function of $\boldsymbol{e}(t)$. Note that V_r is the Lyapunov function that allows us to determine a stabilizing controller in the case of rigid spacecraft.[16] Moreover, V_f is the term necessary to account for the presence of the flexible appendage. Finally, V_d appears in the Lyapunov function V_1 because the estimates $\hat{\boldsymbol{\eta}}$ and $\hat{\boldsymbol{\psi}}$ are used in place of $\boldsymbol{\eta}$ and $\boldsymbol{\psi}$; this further term allows for the determination of the updating laws $\dot{\hat{\boldsymbol{\eta}}}$ and $\dot{\hat{\boldsymbol{\psi}}}$ for the estimates.

Let us now compute the time derivatives of each term along the trajectories of the system (4). Because $\boldsymbol{u}_r(t) \equiv 0$ and $J_r = 0$,

$$\dot{V}_r[\boldsymbol{x}(t),t] = (k_p+k_d)\boldsymbol{e}^T(t)\boldsymbol{\omega}_e(t) + [\boldsymbol{e}(t)+\boldsymbol{\omega}_e(t)]^T \times \left\{\frac{1}{2}J_{10}R(t)\boldsymbol{\omega}_e(t) - \boldsymbol{N}[\boldsymbol{\omega}_e(t),\boldsymbol{\psi}(t),\boldsymbol{\omega}_d(t)] + \delta_0^T[C\boldsymbol{\psi}(t)+K\boldsymbol{\eta}(t)] - \delta_0^T C\delta_0\boldsymbol{\omega}_e(t) + \boldsymbol{u}_g(t) + \Delta_0\boldsymbol{u}_p(t) - J_{10}\dot{\boldsymbol{\omega}}_d(t)\right\}$$

$$\dot{V}_f[\boldsymbol{x}(t)] = [\boldsymbol{\eta}^T(t) \quad \boldsymbol{\psi}^T(t)]P_1 \times \left\{A_c\begin{bmatrix}\boldsymbol{\eta}(t)\\ \boldsymbol{\psi}(t)\end{bmatrix} - B_c\delta_2\boldsymbol{u}_p(t) - A_cB_c\delta_0\boldsymbol{\omega}_e(t) - B_c\delta_0\dot{\boldsymbol{\omega}}_d(t)\right\} \tag{17}$$

$$\dot{V}_d[\boldsymbol{x}(t)] = \begin{bmatrix}\boldsymbol{e}_\eta^T(t) & \boldsymbol{e}_\psi^T(t)\end{bmatrix}P_2\left\{A_c\begin{bmatrix}\boldsymbol{\eta}(t)\\ \boldsymbol{\psi}(t)\end{bmatrix} - B_c\delta_2\boldsymbol{u}_p(t) - A_cB_c\delta_0\boldsymbol{\omega}_e(t) - B_c\delta_0\dot{\boldsymbol{\omega}}_d(t) - \begin{bmatrix}\dot{\hat{\boldsymbol{\eta}}}(t)\\ \dot{\hat{\boldsymbol{\psi}}}(t)\end{bmatrix}\right\}$$

with $\boldsymbol{N}[\boldsymbol{\omega}_e(t),\boldsymbol{\psi}(t),\boldsymbol{\omega}_d(t)]$ as in Eq. (8). Substituting in Eq. (17) the controls (10) and (11), which can be implemented under the hypothesis that both $\boldsymbol{\omega}_d(t)$ and $\dot{\boldsymbol{\omega}}_d(t)$ are bounded, i.e., $\|\boldsymbol{\omega}_d(t)\|, \|\dot{\boldsymbol{\omega}}_d(t)\| \in L_\infty[0,\infty)$, $\dot{V}_1[\boldsymbol{x}(t),t]$, takes the form

$$\begin{aligned}\dot{V}_1[\boldsymbol{x}(t),t] &= -k_p\|\boldsymbol{e}(t)\|^2 - k_d\|\boldsymbol{\omega}_e(t)\|^2 \\ &+ [\boldsymbol{\eta}^T(t) \quad \boldsymbol{\psi}^T(t)]P_1\bar{A}_c\begin{bmatrix}\boldsymbol{\eta}(t)\\ \boldsymbol{\psi}(t)\end{bmatrix} \\ &- [\boldsymbol{\eta}^T(t) \quad \boldsymbol{\psi}^T(t)]P_1A_cB_c\delta_0\boldsymbol{\omega}_e(t) \\ &- [\boldsymbol{\eta}^T(t) \quad \boldsymbol{\psi}^T(t)]P_1B_c\delta_0\dot{\boldsymbol{\omega}}_d(t) + \begin{bmatrix}\boldsymbol{e}_\eta^T(t) & \boldsymbol{e}_\psi^T(t)\end{bmatrix} \\ &\times \left(P_2\left\{\bar{A}_c\begin{bmatrix}\boldsymbol{\eta}(t)\\ \boldsymbol{\psi}(t)\end{bmatrix} + B_c\delta_2\delta_2^T(\lambda_1 I \quad \lambda_2 I)\begin{bmatrix}\boldsymbol{e}_\eta(t)\\ \boldsymbol{e}_\psi(t)\end{bmatrix} - A_cB_c\delta_0\boldsymbol{\omega}_e(t) - B_c\delta_0\dot{\boldsymbol{\omega}}_d(t) - \begin{bmatrix}\dot{\hat{\boldsymbol{\eta}}}(t)\\ \dot{\hat{\boldsymbol{\psi}}}(t)\end{bmatrix}\right\} \right. \\ &+ \left\{\begin{matrix}K\delta_0 \\ \delta_0[\tilde{\boldsymbol{\omega}}_e(t)+\tilde{\boldsymbol{\omega}}_d(t)] + C\delta_0\end{matrix}\right\}[\boldsymbol{e}(t)+\boldsymbol{\omega}_e(t)] \\ &\left. + \begin{pmatrix}\lambda_1 I\\ \lambda_2 I\end{pmatrix}\delta_2\delta_2^T B_c^T P_1\begin{pmatrix}\boldsymbol{\eta}\\ \boldsymbol{\psi}\end{pmatrix}\right)\end{aligned}$$

Now the updating laws (9) ensure that

$$\begin{aligned}\dot{V}_1[\boldsymbol{x}(t),t] &= -k_p\|\boldsymbol{e}(t)\|^2 - k_d\|\boldsymbol{\omega}_e(t)\|^2 \\ &- [\boldsymbol{\eta}^T(t) \quad \boldsymbol{\psi}^T(t)]Q_1\begin{bmatrix}\boldsymbol{\eta}(t)\\ \boldsymbol{\psi}(t)\end{bmatrix} \\ &- [\boldsymbol{\eta}^T(t) \quad \boldsymbol{\psi}^T(t)]P_1A_cB_c\delta_0\boldsymbol{\omega}_e(t) \\ &- [\boldsymbol{\eta}^T(t) \quad \boldsymbol{\psi}^T(t)]P_1B_c\delta_0\dot{\boldsymbol{\omega}}_d(t) - \begin{bmatrix}\boldsymbol{e}_\eta^T(t) & \boldsymbol{e}_\psi^T(t)\end{bmatrix} \\ &\times \left[Q_2 - \begin{pmatrix}\lambda_1 I\\ \lambda_2 I\end{pmatrix}\delta_2\delta_2^T B_c^T P_1\right]\begin{bmatrix}\boldsymbol{e}_\eta(t)\\ \boldsymbol{e}_\psi(t)\end{bmatrix}\end{aligned}$$

where Eqs. (12) were used. Finally, with the choice (13), we obtain

$$\begin{aligned}\dot{V}_1[\boldsymbol{x}(t),t] &= -\boldsymbol{x}^T(t)Q\boldsymbol{x}(t) - [\boldsymbol{\eta}^T(t) \quad \boldsymbol{\psi}^T(t)]P_1B_c\delta_0\dot{\boldsymbol{\omega}}_d(t) \\ &\le -\lambda_m\|\boldsymbol{x}(t)\|^2 + \alpha\|\dot{\boldsymbol{\omega}}_d(t)\|\|\boldsymbol{x}(t)\|\end{aligned}$$

with

$$Q = \begin{pmatrix} k_pI & 0 & 0 & 0 & 0 & 0 \\ 0 & k_dI & M_1^T & M_2^T & 0 & 0 \\ 0 & M_1 & \lambda_\eta I & 0 & 0 & 0 \\ 0 & M_2 & 0 & \lambda_\psi I & 0 & 0 \\ 0 & 0 & 0 & 0 & \lambda_{e_\eta} I & 0 \\ 0 & 0 & 0 & 0 & 0 & \lambda_{e_\psi} I \end{pmatrix}$$

$$M_1 = -\tfrac{1}{2}(P_{11} - P_{12}C)\delta_0, \qquad M_2 = -\tfrac{1}{2}\left(P_{12}^T - P_{13}C\right)\delta_0$$

and $\lambda_m = \min\sigma(Q)$ and $\alpha = \|P_1A_cB_c\delta_0\|$. The matrix Q is positive definite because

$$\begin{aligned}k_dI - \begin{pmatrix}M_1^T & M_2^T\end{pmatrix}\begin{bmatrix}(1/\lambda_\eta)I & 0\\ 0 & (1/\lambda_\psi)I\end{bmatrix}\begin{pmatrix}M_1\\ M_2\end{pmatrix} &= k_dI - \frac{1}{4}\left[\frac{\delta_0^T\left(P_{11}-CP_{12}^T\right)(P_{11}-P_{12}C)\delta_0}{\lambda_\eta}\right. \\ &\left. + \frac{\delta_0^T\left(P_{12}-CP_{13}^T\right)\left(P_{12}^T-P_{13}C\right)\delta_0}{\lambda_\psi}\right] > 0\end{aligned} \tag{18}$$

for appropriate values of k_d, λ_η, λ_ψ, and, therefore, $\lambda_m > 0$.

Integrating both sides and using the Schwarz inequality

$$\left[\int_a^b y(\tau)z(\tau)\,\mathrm{d}\tau\right]^2 \le \int_a^b y^2(\tau)\,\mathrm{d}\tau\int_a^b z^2(\tau)\,\mathrm{d}\tau$$

we have

$$\begin{aligned}V_1[\boldsymbol{x}(t),t] - V_1[\boldsymbol{x}(0),0] &\le -\lambda_m\int_0^t\|\boldsymbol{x}(\tau)\|^2\,\mathrm{d}\tau + \alpha\int_0^t\|\dot{\boldsymbol{\omega}}_d(\tau)\|\|\boldsymbol{x}(\tau)\|\,\mathrm{d}\tau \\ &\le -\lambda_m\|\boldsymbol{x}\|_2^2 + \alpha\|\dot{\boldsymbol{\omega}}_d\|_2\|\boldsymbol{x}\|_2\end{aligned} \tag{19}$$

where $\|\cdot\|_2$ denotes the L_2 norm. Moreover, because $V_1[\boldsymbol{x}(t),t] \ge 0$,

$$\lambda_m\|\boldsymbol{x}\|_2^2 - \alpha\|\dot{\boldsymbol{\omega}}_d\|_2\|\boldsymbol{x}\|_2 \le V_1[\boldsymbol{x}(0),0] - V_1[\boldsymbol{x}(t),t] \le V_1[\boldsymbol{x}(0),0]$$

and supposing that $\dot{\boldsymbol{\omega}}_d(t) \in L_2[0,\infty) \cap L_\infty[0,\infty)$, we obtain the bound

$$\|\boldsymbol{x}\|_2 \le \frac{1}{\sqrt{\lambda_m}}\left\{V_1[\boldsymbol{x}(0),0] + \frac{\alpha^2}{4\lambda_m}\|\dot{\boldsymbol{\omega}}_d\|_2^2\right\}^{\frac{1}{2}} + \frac{\alpha}{2\lambda_m}\|\dot{\boldsymbol{\omega}}_d\|_2$$

Hence, $\boldsymbol{x}(t) \in L_2[0,\infty)$. From this and relationship (19) it follows that, under the hypothesis given for $\boldsymbol{\omega}_d(t)$, $V_1[\boldsymbol{x}(t),t]$ is uniformly bounded in t along the solution trajectories, i.e.,

$$\lim_{t\to\infty} V_1[\boldsymbol{x}(t),t] < \infty$$

This implies that $\boldsymbol{x}(t)$ is uniformly bounded. Moreover, from Eq. (4) it is also clear that $\dot{\boldsymbol{x}}(t)$ is uniformly bounded, and this implies that $\boldsymbol{x}(t)$ is uniformly continuous. Therefore, because $\boldsymbol{x}(t)$ is a uniformly continuous function in $L_2[0, \infty)$, from the Barbalat theorem[32] we have that

$$\lim_{t\to\infty} \boldsymbol{x}(t) = 0, \qquad \lim_{t\to\infty} \boldsymbol{y}_1(t) = 0, \qquad \lim_{t\to\infty} \boldsymbol{y}_2(t) = 0$$

Hence, the proposed controller fulfills the control objectives.

Remark 2. If the active actuators are absent, i.e., $\lambda_1 = \lambda_2 = 0$ in Eqs. (9–11), theorem 1 still retains its validity. From the expression of $\bar{A}_c$, it is clear that the role of the active control is to increase the damping and stiffness of the flexible boom. Note also that the structure damping matrix is $C + \lambda_2\delta_2\delta_2^T$. Hence, if the internal damping is negligible, i.e., if $C = 0$, the damping matrix is simply $\lambda_2\delta_2\delta_2^T$. This matrix has some of its eigenvalues in the origin; they correspond to the torsional deformation. Physically, this is because the piezoelectric films can increase the stiffness linked with the deformations in the x and y directions, but (ideally) not the stiffness related to the torsion. This means that the controller of theorem 1 fulfills the control objectives but does not ensure asymptotic stability because it does not damp the torsional deformations. This could be a drawback in some practical cases, whereas in others it could be an acceptable behavior. □

Remark 3. The control (10) is nonlinear because of the gyroscopic term. Note that for rest-to-rest maneuvers, where $\boldsymbol{\omega}_d(t) \equiv 0$, this term can be eliminated. In fact, in this case the dynamic controller could be derived by using the Lyapunov function

$$V_r[\boldsymbol{x}(t)] = k_p\{[e_0(t) - 1]^2 + \boldsymbol{e}^T(t)\boldsymbol{e}(t)\} + \tfrac{1}{2}\boldsymbol{\omega}_e(t)J_{10}\boldsymbol{\omega}_e(t)$$

where

$$\dot{V}_r[\boldsymbol{x}(t)] = \boldsymbol{\omega}_e^T(t)\Big\{k_p\boldsymbol{e}(t) + \delta_0^T[C\boldsymbol{\psi}(t) + K\boldsymbol{\eta}(t)] - \delta_0^T C\delta_0\boldsymbol{\omega}_e(t) + \boldsymbol{u}_g(t) + \Delta_0\boldsymbol{u}_p(t)\Big\}$$

This leads to the following controller:

$$\begin{bmatrix}\dot{\hat{\boldsymbol{\eta}}}(t)\\ \dot{\hat{\boldsymbol{\psi}}}(t)\end{bmatrix} = \bar{A}_c\begin{bmatrix}\hat{\boldsymbol{\eta}}(t)\\ \hat{\boldsymbol{\psi}}(t)\end{bmatrix} - A_cB_c\delta_0\boldsymbol{\omega}_e(t) - B_c\delta_2\boldsymbol{u}_{p1}(t) + P_2^{-1}\begin{pmatrix}\lambda_1 I\\ \lambda_2 I\end{pmatrix}\delta_2\delta_2^TB_c^TP_1\begin{bmatrix}\hat{\boldsymbol{\eta}}(t)\\ \hat{\boldsymbol{\psi}}(t)\end{bmatrix}$$

$$\boldsymbol{u}_g(t) = -k_p\boldsymbol{e}(t) - k_d\boldsymbol{\omega}_e(t) - \delta_0^T[C\hat{\boldsymbol{\psi}}(t) + K\hat{\boldsymbol{\eta}}(t)] + \delta_0^TC\delta_0\boldsymbol{\omega}_e(t) - \Delta_0\boldsymbol{u}_{p1}(t)$$

$$\boldsymbol{u}_p(t) = \boldsymbol{u}_{p1}(t)$$

which fulfills the control objectives because

$$\dot{V}_1[\boldsymbol{x}(t)] = -k_d\|\boldsymbol{\omega}_e(t)\|^2 - [\boldsymbol{\eta}^T(t) \quad \boldsymbol{\psi}^T(t)]Q_1\begin{bmatrix}\boldsymbol{\eta}(t)\\ \boldsymbol{\psi}(t)\end{bmatrix} - \begin{bmatrix}\boldsymbol{e}_\eta^T(t) & \boldsymbol{e}_\psi^T(t)\end{bmatrix}\left[Q_2 - \begin{pmatrix}\lambda_1 I\\ \lambda_2 I\end{pmatrix}\delta_2\delta_2^TB_c^TP_1\right]\begin{bmatrix}\boldsymbol{e}_\eta(t)\\ \boldsymbol{e}_\psi(t)\end{bmatrix} \le 0$$

(La Salle theorem, Ref. 33). □

B. Reaction Wheels Control Mode

When reaction wheels are present, different situations are possible. In fact, we can have maneuvers performed by a combined gas jet and reaction wheel action, or maneuvers performed by gas jets only, or maneuvers obtained with reaction wheels only. Hereinafter we analyze these three cases and we give the controllers that solve the control problem, as summarized in the following theorem.

Theorem 2. Under the hypotheses given in theorem 1 for the reference $\boldsymbol{\omega}_d(t)$, the following dynamic controllers solve the control problem for system (4) in the presence of reaction wheels.

Stabilization via gas jets and reaction wheels:

$$\begin{bmatrix}\dot{\hat{\boldsymbol{\eta}}}(t)\\ \dot{\hat{\boldsymbol{\psi}}}(t)\end{bmatrix} = \boldsymbol{\Gamma}[\boldsymbol{\omega}(t), \hat{\boldsymbol{\eta}}(t), \hat{\boldsymbol{\psi}}(t), \boldsymbol{\omega}_d(t)]$$

$$\begin{aligned}\boldsymbol{u}_g(t) &= -k_p\boldsymbol{e}(t) - k_d\boldsymbol{\omega}_e(t) - \tfrac{1}{2}J_{10}R(t)\boldsymbol{\omega}_e(t)\\ &\quad + \boldsymbol{N}[\boldsymbol{\omega}_e(t), \boldsymbol{\Omega}(t), \hat{\boldsymbol{\psi}}(t), \boldsymbol{\omega}_d(t)] - \delta_0^T[C\hat{\boldsymbol{\psi}}(t) + K\hat{\boldsymbol{\eta}}(t)]\\ &\quad + \delta_0^TC\delta_0\boldsymbol{\omega}_e(t) - \Delta_0\boldsymbol{u}_{p1}(t) + (J_{10} + J_r)\dot{\boldsymbol{\omega}}_d(t)\\ \boldsymbol{u}_r(t) &= -k_r\boldsymbol{\Omega}(t) + J_r\dot{\boldsymbol{\omega}}_d(t), \qquad \boldsymbol{u}_p(t) = \boldsymbol{u}_{p1}(t)\end{aligned} \tag{20}$$

Stabilization via gas jets:

$$\begin{bmatrix}\dot{\hat{\boldsymbol{\eta}}}(t)\\ \dot{\hat{\boldsymbol{\psi}}}(t)\end{bmatrix} = \boldsymbol{\Gamma}[\boldsymbol{\omega}(t), \hat{\boldsymbol{\eta}}(t), \hat{\boldsymbol{\psi}}(t), \boldsymbol{\omega}_d(t)]$$

$$\begin{aligned}\boldsymbol{u}_g(t) &= -k_p\boldsymbol{e}(t) - k_d\boldsymbol{\omega}_e(t) - \tfrac{1}{2}J_{10}R(t)\boldsymbol{\omega}_e(t)\\ &\quad + \boldsymbol{N}[\boldsymbol{\omega}_e(t), \boldsymbol{\Omega}(t), \hat{\boldsymbol{\psi}}(t), \boldsymbol{\omega}_d(t)] - \delta_0^T[C\hat{\boldsymbol{\psi}}(t) + K\hat{\boldsymbol{\eta}}(t)]\\ &\quad + \delta_0^TC\delta_0\boldsymbol{\omega}_e(t) - \Delta_0\boldsymbol{u}_{p1}(t) + J_{10}\dot{\boldsymbol{\omega}}_d(t)\\ \boldsymbol{u}_r(t) &\equiv 0, \qquad \boldsymbol{u}_p(t) = \boldsymbol{u}_{p1}(t)\end{aligned} \tag{21}$$

Stabilization via reaction wheels:

$$\begin{bmatrix}\dot{\hat{\boldsymbol{\eta}}}(t)\\ \dot{\hat{\boldsymbol{\psi}}}(t)\end{bmatrix} = \boldsymbol{\Gamma}[\boldsymbol{\omega}(t), \hat{\boldsymbol{\eta}}(t), \hat{\boldsymbol{\psi}}(t), \boldsymbol{\omega}_d(t)]$$

$$\begin{aligned}\boldsymbol{u}_g(t) &\equiv 0\\ \boldsymbol{u}_r(t) &= k_p\boldsymbol{e}(t) + k_d\boldsymbol{\omega}_e(t) + \tfrac{1}{2}J_{10}R(t)\boldsymbol{\omega}_e(t)\\ &\quad - \boldsymbol{N}[\boldsymbol{\omega}_e(t), \boldsymbol{\Omega}(t), \hat{\boldsymbol{\psi}}(t), \boldsymbol{\omega}_d(t)] + \delta_0^T[C\hat{\boldsymbol{\psi}}(t) + K\hat{\boldsymbol{\eta}}(t)]\\ &\quad - \delta_0^TC\delta_0\boldsymbol{\omega}_e(t) + \Delta_0\boldsymbol{u}_{p1}(t) - J_{10}\dot{\boldsymbol{\omega}}_d(t)\\ \boldsymbol{u}_p(t) &= \boldsymbol{u}_{p1}(t)\end{aligned} \tag{22}$$

with J_{10}, $\boldsymbol{\Gamma}[\boldsymbol{\omega}(t), \hat{\boldsymbol{\eta}}(t), \hat{\boldsymbol{\psi}}(t), \boldsymbol{\omega}_d(t)]$, and $\boldsymbol{u}_{p1}(t)$ defined in Eqs. (5), (9), and (11); and P_1 and P_2 solutions of Eqs. (12) and (13); and

$$\boldsymbol{N}[\boldsymbol{\omega}_e(t), \boldsymbol{\Omega}(t), \hat{\boldsymbol{\psi}}(t), \boldsymbol{\omega}_d(t)] = [\tilde{\boldsymbol{\omega}}_e(t) + \tilde{\boldsymbol{\omega}}_d(t)] \times \Big[\Big(J_0 - \delta_0^T\delta_0\Big)\boldsymbol{\omega}_e(t) + J_r\boldsymbol{\Omega}(t) + \delta_0^T\hat{\boldsymbol{\psi}}(t) + J_0\boldsymbol{\omega}_d(t)\Big]$$

□

Remark 4. Controllers (20–22) all ensure the solution of the control problem. The difference among these controllers is that although the stabilization via gas jets and reaction wheels guarantees that also the reaction wheels angular velocity $\boldsymbol{\Omega}(t)$ goes to zero, the stabilization via gas jets or via reaction wheels determines a simply bounded angular velocity $\boldsymbol{\Omega}(t)$. □

To prove this statement, we have considered, first, the stabilization via gas jets and reaction wheels and the Lyapunov function,

$$V_2[\boldsymbol{x}(t), \boldsymbol{\Omega}(t), t] = V_1[\boldsymbol{x}(t), t] + \tfrac{1}{2}[\boldsymbol{\omega}_e(t) + \boldsymbol{\Omega}(t)]^TJ_r[\boldsymbol{\omega}_e(t) + \boldsymbol{\Omega}(t)]$$

which is similar to the function $V_1[\boldsymbol{x}(t), t]$, as defined in Sec. III.A, with a small modification taking into account the presence of the reaction wheels. Therefore,

$$\begin{aligned}\dot{V}_2[\boldsymbol{x}(t), \boldsymbol{\Omega}(t), t] &= (k_p + k_d)\boldsymbol{e}^T(t)\boldsymbol{\omega}_e(t) + [\boldsymbol{e}(t) + \boldsymbol{\omega}_e(t)]^T\\ &\quad \times \Big\{\tfrac{1}{2}J_{10}R(t)\boldsymbol{\omega}_e(t) - \boldsymbol{N}[\boldsymbol{\omega}_e(t), \boldsymbol{\Omega}(t), \boldsymbol{\psi}(t), \boldsymbol{\omega}_d(t)]\\ &\quad + \delta_0^T[C\boldsymbol{\psi}(t) + K\boldsymbol{\eta}(t)] - \delta_0^TC\delta_0\boldsymbol{\omega}_e(t) + \boldsymbol{u}_g(t) - \boldsymbol{u}_r(t)\\ &\quad + \Delta_0\boldsymbol{u}_p(t) - J_{10}\dot{\boldsymbol{\omega}}_d(t)\Big\} + \dot{V}_f[\boldsymbol{x}(t)] + \dot{V}_d[\boldsymbol{x}(t)]\\ &\quad + [\boldsymbol{\omega}_e(t) + \boldsymbol{\Omega}(t)]^T[\boldsymbol{u}_r(t) - J_r\dot{\boldsymbol{\omega}}_d(t)]\end{aligned} \tag{23}$$

where $\dot{V}_f[\boldsymbol{x}(t)]$ and $\dot{V}_d[\boldsymbol{x}(t)]$ are as in Eq. (17).

Hence, the control problem can be solved by means of the controller (20), because

$$\dot{V}_2[\boldsymbol{x}(t), \boldsymbol{\Omega}(t), t] = -\bar{\boldsymbol{x}}(t)\bar{Q}\bar{\boldsymbol{x}}(t) + \alpha\|\dot{\boldsymbol{\omega}}_d(t)\|\|\bar{\boldsymbol{x}}(t)\|$$

$$\leq -\bar{\lambda}_m\|\bar{\boldsymbol{x}}(t)\|^2 + \alpha\|\dot{\boldsymbol{\omega}}_d(t)\|\|\bar{\boldsymbol{x}}(t)\|$$

with $\bar{\boldsymbol{x}}(t) = [\boldsymbol{\Omega}^T(t) \quad \boldsymbol{x}^T(t)]^T$,

$$\bar{Q} = \begin{bmatrix} k_r I & -(k_r/2)I & 0 & 0 & 0 & 0 & 0 \\ -(k_r/2)I & k_p I & 0 & 0 & 0 & 0 & 0 \\ 0 & 0 & k_d I & M_1^T & M_2^T & 0 & 0 \\ 0 & 0 & M_1 & \lambda_\eta I & 0 & 0 & 0 \\ 0 & 0 & M_2 & 0 & \lambda_\psi I & 0 & 0 \\ 0 & 0 & 0 & 0 & 0 & \lambda_{e_\eta} I & 0 \\ 0 & 0 & 0 & 0 & 0 & 0 & \lambda_{e_\psi} I \end{bmatrix}$$

$\bar{\lambda}_m = \min\sigma(\bar{Q})$, $\boldsymbol{x}(t)$, M_1, M_2, and α defined in Sec. III.A. Note that $\bar{Q}$ is positive definite because

$$\begin{bmatrix} k_r I & -(k_r/2)I \\ -(k_r/2)I & k_p I \end{bmatrix} > 0$$

if $0 < k_r < 4k_p$ and Eq. (18) is true for appropriate k_d, λ_η, and λ_ψ. Therefore, under the same hypotheses given on the desired angular velocity and with the same technique used in Sec. III.A, according to the Barbalat theorem it follows that the control objectives are verified, with

$$\lim_{t\to\infty} \boldsymbol{\Omega}(t) = 0$$

Second, let us consider the stabilization problem with gas jets only [$\boldsymbol{u}_r(t) \equiv 0$]. The candidate Lyapunov function is again similar to $V_1[\boldsymbol{x}(t), t]$ given in Sec. III.A; to obtain easier computations, the term that considers the reaction wheels is slightly different from that used in $V_2[\boldsymbol{x}(t), t]$. This function has the form

$$V_3[\boldsymbol{x}(t), \boldsymbol{\Omega}(t), t] = V_1[\boldsymbol{x}(t), t] + \tfrac{1}{2}\boldsymbol{\chi}(t)^T\boldsymbol{\chi}(t)$$

with $\boldsymbol{\chi}(t) = \boldsymbol{\omega}_e(t) + \boldsymbol{\Omega}(t) + \boldsymbol{\omega}_d(t) = \boldsymbol{\omega}(t) + \boldsymbol{\Omega}(t)$, which is such that [see Eq. (2)]

$$\dot{V}_3[\boldsymbol{x}(t), \boldsymbol{\Omega}(t), t] = \dot{V}_1[\boldsymbol{x}(t), t] \leq -\lambda_m\|\boldsymbol{x}(t)\|^2 + \alpha\|\dot{\boldsymbol{\omega}}_d(t)\|\|\boldsymbol{x}(t)\|$$

because $\boldsymbol{u}_r(t) \equiv 0$, with λ_m, $\boldsymbol{x}(t)$, and α as in Sec. III.A. Using the same arguments and Eq. (21) controls and updating laws, we deduce that

$$\lim_{t\to\infty} \boldsymbol{x}(t) = 0$$

and the solution of the control problem, with

$$V_3[\boldsymbol{x}(t), \boldsymbol{\Omega}(t), t] \leq V_3[\boldsymbol{x}(0), \boldsymbol{\Omega}(0), 0] - \lambda_m\|\boldsymbol{x}\|_2^2 + \alpha\|\dot{\boldsymbol{\omega}}_d\|_2\|\boldsymbol{x}\|_2$$

This last relationship implies that $\boldsymbol{\Omega}(t)$ remains uniformly bounded in t.

Finally, let us consider the case in which only reaction wheels are used [$\boldsymbol{u}_g(t) \equiv 0$]. In this case, using

$$V_4[\boldsymbol{x}(t), \boldsymbol{\Omega}(t), t] = V_1[\boldsymbol{x}(t), t] + \tfrac{1}{2}\boldsymbol{\xi}^T(t)\boldsymbol{\xi}(t)$$

where

$$\boldsymbol{\xi}(t) = \left(J_0 - \delta_0^T\delta_0\right)\boldsymbol{\omega}_e(t) + J_r\boldsymbol{\Omega}(t) + \delta_0^T\boldsymbol{\psi}(t) + J_0\boldsymbol{\omega}_d(t)$$

$$= J_0\boldsymbol{\omega}(t) + J_r\boldsymbol{\Omega}(t) + \delta_0^T\dot{\boldsymbol{\eta}}(t)$$

we have

$$\dot{V}_4[\boldsymbol{x}(t), \boldsymbol{\Omega}(t), t] = (k_p + k_d)\boldsymbol{e}^T(t)\boldsymbol{\omega}_e(t) + [\boldsymbol{e}(t) + \boldsymbol{\omega}_e(t)]^T$$

$$\times \left\{\tfrac{1}{2}J_{10}R(t)\boldsymbol{\omega}_e(t) - \boldsymbol{N}[\boldsymbol{\omega}_e(t), \boldsymbol{\Omega}(t), \boldsymbol{\psi}(t), \boldsymbol{\omega}_d(t)]\right.$$

$$+ \delta_0^T[C\boldsymbol{\psi}(t) + K\boldsymbol{\eta}(t)] - \delta_0^T C\delta_0\boldsymbol{\omega}_e(t) - \boldsymbol{u}_r(t)$$

$$\left. + \Delta_0\boldsymbol{u}_p(t) - J_{10}\dot{\boldsymbol{\omega}}_d(t)\right\} + \dot{V}_f[\boldsymbol{x}(t)] + \dot{V}_d[\boldsymbol{x}(t)]$$

where $\dot{V}_f[\boldsymbol{x}(t)]$ and $\dot{V}_d[\boldsymbol{x}(t)]$ are as in Eq. (17), because $\boldsymbol{\xi}^T(t)\dot{\boldsymbol{\xi}}(t) = \boldsymbol{\xi}^T(t)[-\tilde{\boldsymbol{\omega}}(t)\boldsymbol{\xi}(t) + \boldsymbol{u}_g(t)] = 0$ [see Eq. (2)]. Therefore, with the controller (22) we have again

$$\dot{V}_4[\boldsymbol{x}(t), \boldsymbol{\Omega}(t), t] \leq -\lambda_m\|\boldsymbol{x}(t)\|^2 + \alpha\|\dot{\boldsymbol{\omega}}_d(t)\|\|\boldsymbol{x}(t)\|$$

and it is straightforward to deduce that the control problem is solved. Because

$$V_4[\boldsymbol{x}(t), \boldsymbol{\Omega}(t), t] \leq V_4[\boldsymbol{x}(0), \boldsymbol{\Omega}(0), 0] - \lambda_m\|\boldsymbol{x}\|_2^2 + \alpha\|\dot{\boldsymbol{\omega}}_d\|_2\|\boldsymbol{x}\|_2$$

$\boldsymbol{\Omega}(t)$ is uniformly bounded in t.

Remark 5. For the controls of theorem 2 the same observation made in remark 3 is valid. □

IV. Simulation Results

An accurate spacecraft model has been implemented on a digital computer to test the controllers designed in the preceding section. These controllers were derived on the basis of the simplified model (4). The presence of a higher order of elastic mode and of time-varying terms in the spacecraft model used for simulation, not considered in Eq. (4), and the performances obtained and hereinafter illustrated, represent a spillover robustness test for the proposed controllers.

The appendage is presumed to be composed of aluminum, 1.5 m long and with square section (10^{-4} m^2), carrying a payload of 1 kg. Two bending modes are considered in the plane perpendicular to the boom, and there are two torsional modes. The piezoelectric films are made of vinylidene fluoride (PVDF) bonded to the appendage by bounding layers made of Isotac.[23] The spacecraft parameters are summarized in the Appendix, along with those characterizing the flexible appendage and the piezoelectric and bounding layers. If E_p, E_{bl}, and E_b and t_p, t_{bl}, and t_b are Young's modulus of elasticity and piezoelectric layer, bounding layer, and the beam thicknesses, d_p is the piezoelectric charge constant, and b_b is the beam width (equal to t_b in our case); the constants c_{px} and c_{py}, related to the bending moments generated by the piezoelectric films, are given by[23]

$$c_{px} = c_{py} = \frac{d_p b_b E_p[E_{\mathrm{bl}}t_{\mathrm{bl}}(t_p + t_{\mathrm{bl}}) + E_b t_b(t_p + 2t_{\mathrm{bl}} + t_b)]}{2(E_p t_p + E_{\mathrm{bl}}t_{\mathrm{bl}} + E_b t_b)}$$

In the following simulations the situation described in theorem 1 is considered (absence of reaction wheels), and a tracking maneuver is described by the following reference quaternions, expressing the attitude of the desired reference frame $\mathcal{R}_d$:

$$q_{r0}(t) = \cos\frac{\Phi(t)}{2}, \qquad \begin{bmatrix} q_{r1}(t) \\ q_{r2}(t) \\ q_{r3}(t) \end{bmatrix} = \begin{bmatrix} \cos(0.37t) \\ \sin(0.37t) \\ 0 \end{bmatrix} \sin\frac{\Phi(t)}{2}$$

$$\Phi(t) = \sin(0.02t)$$

Note that if Φ were constant, these quaternions would correspond to a precession around the z axis; the amplitude of the cone described during the precession motion is proportional to the angle Φ. Hence, it is clear that if Φ varies sinusoidally, as in our case, one obtains a spiral maneuver starting from the initial spacecraft attitude. As $\Phi(t)$ increases, the spiral enlarges, whereas as $\Phi(t)$ decreases, the spiral converges to the initial attitude. This maneuver, although quite unusual and probably without an immediate application in practical cases, could be interesting as a particular scanning maneuver of a region of the sky.

For simplicity the initial error quaternions $\boldsymbol{e}(0)$, error angular velocity $\boldsymbol{\omega}_e(0)$, and modal displacements and velocities $\boldsymbol{\eta}(0)$ and $\boldsymbol{z}(0)$ are presumed zero, but the following results apply without any substantial difference when these quantities differ from zero for sufficiently small quantities.

The parameters of the dynamic controller are

$$k_p = 300, \qquad k_d = 600, \qquad \lambda_1 = \lambda_2 = 10^{12}$$

$$\lambda_\eta = \lambda_\psi = 10^2, \qquad \lambda_{e_\eta} = \lambda_{e_\psi} = 10^3$$

and the chosen initial conditions for the estimated variables are $\hat{\boldsymbol{\eta}}(0) = 0$ and $\hat{\psi}(0) = 0$.

Simulations have been rendered more realistic by considering saturation on the inputs. The fixed maximum values are $u_{g,\max} = 30\,\text{Nm}$ and $u_{p,\max} = 1400\,\text{V}$, with the latter value related to the piezoelectric used.[23]

As stressed in Ref. 24, simulations show that the role of the piezoelectric is to suppress small displacements during the tracking. This not only results in an increase in pointing precision but can also prevent unstable behaviors of the system. In fact, the presence of saturation on the inputs can lead to amplified oscillations and eventually to instability, as described by Figs. 2–4, which refer to the case of absence of piezoelectric actuators. The great activity of the inputs and their discontinuity (Fig. 3) amplify tip displacements (Fig. 4) and error quaternions (Fig. 2).

On the other hand, when piezoelectric actuators are present, these small vibrations during tracking maneuvers can be successfully attenuated. Because of the damping of these vibrations, with the active control it is possible to more accurately track the desired trajectory, as shown by Figs. 5–10. In fact, the other actuators are now less active (the gas jets, Fig. 8) and the resulting control action is more precise due to the piezoelectric contribution (Fig. 9). Comparison of Fig. 3, where the thrusters are almost always firing, with Fig. 8 helps us to understand the cost benefit, in terms of fuel consumption, of using piezoelectric dampers. The behavior of the elastic oscillations takes advantage of this increase of control accuracy (Fig. 10), and the tracking errors are less pronounced, as shown by Fig. 5 and by Figs. 6 and 7. Moreover, the x and y deflections are now almost equal; this does not appear in the absence of active damping (Fig. 4)

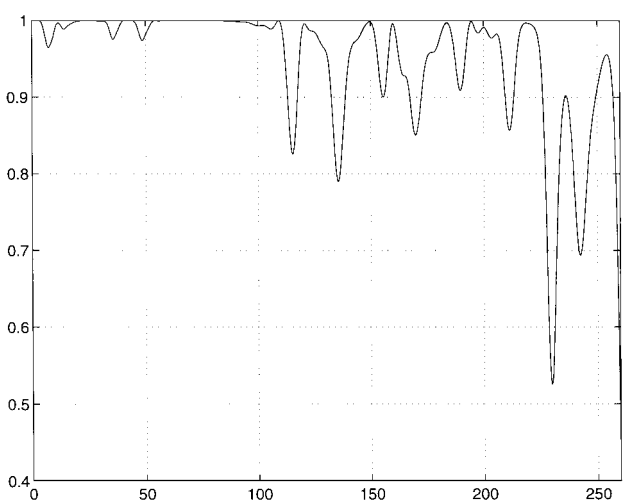

Fig. 2 Error quaternion $e_0(t)$.

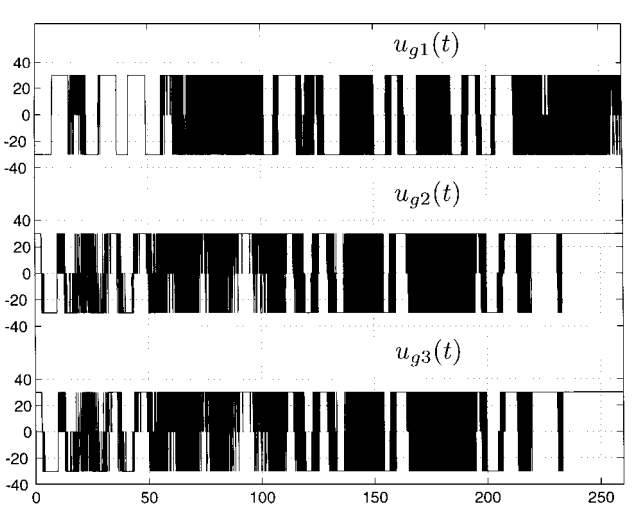

Fig. 3 Inputs $u_{g1}(t)$, $u_{g2}(t)$, and $u_{g3}(t)$, newton meters.

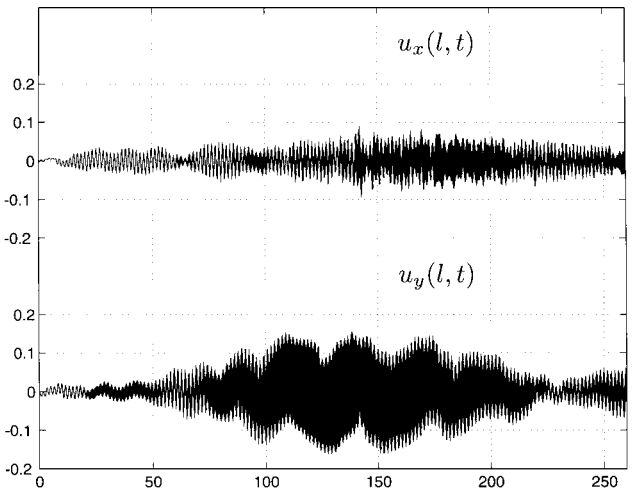

Fig. 4 Tip displacements $u_x(l,t)$ and $u_y(l,t)$, meters.

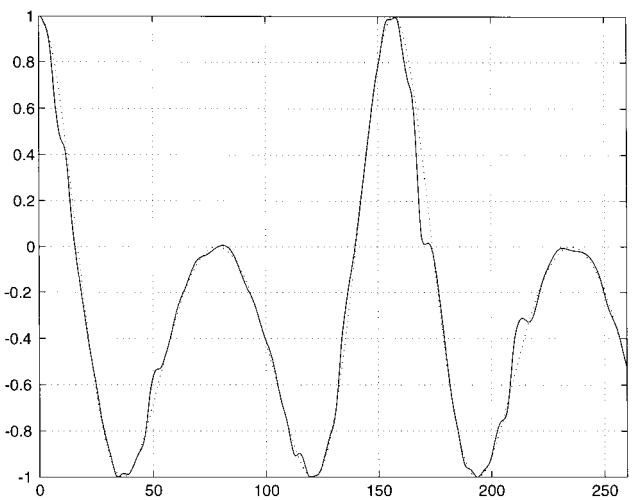

Fig. 5 Quaternions $q_0(t)$ and $q_{0r}(t)$.

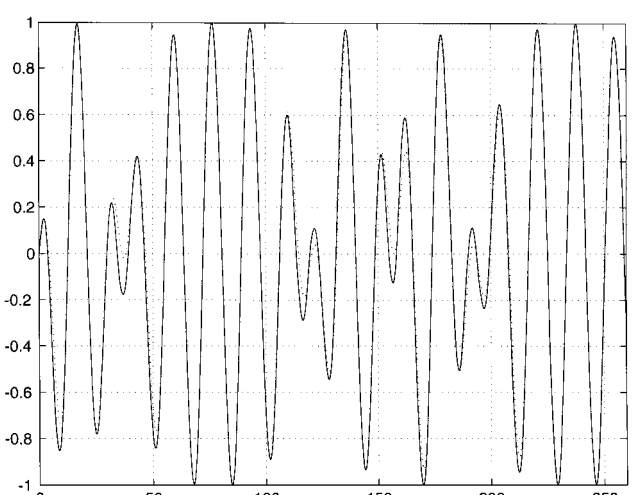

Fig. 6 Quaternions $q_1(t)$ and $q_{1r}(t)$.

inasmuch as the control action, carried2 out by the thrusters, is more imprecise because of the saturation limits and their discontinuous nature.

Results similar to those presented can be obtained when we consider the situations presented in theorem 2, when the gain k_r (and/or the saturation value $u_{r,\max}$) for the reaction wheels is low compared with the control activity necessary to suppress the (fast) elastic deflections.

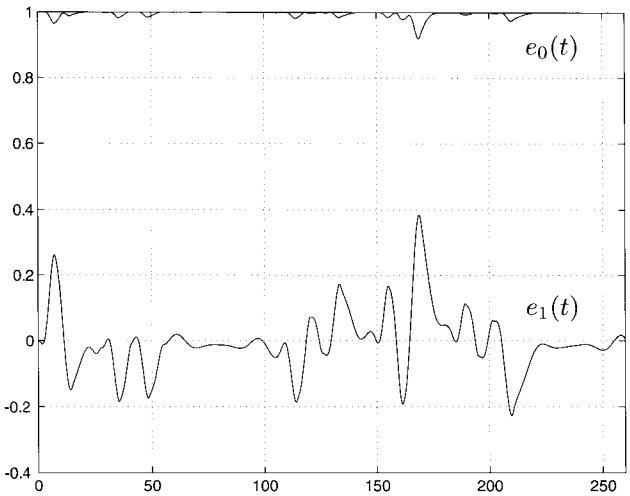

Fig. 7 Error quaternions $e_0(t)$ and $e_1(t)$.

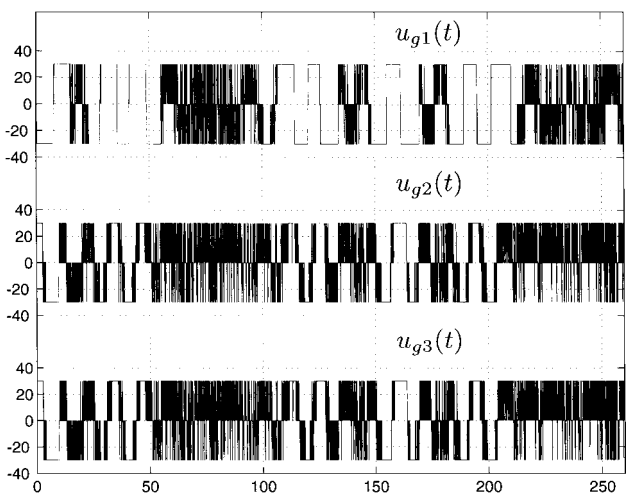

Fig. 8 Inputs $u_{g1}(t)$, $u_{g2}(t)$, and $u_{g3}(t)$, newton meters.

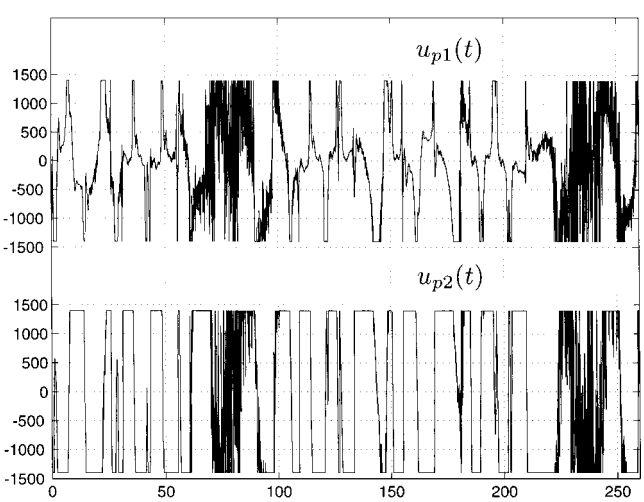

Fig. 9 Piezoelectric inputs $u_{p1}(t)$ and $u_{p2}(t)$, volts.

Note that, if the control law is applied to the simplified model (4), used to derive the control, the unstable behavior shown in Fig. 2 does not appear. It is clear that this is due to the effects of the modal dynamics and time-varying terms, absent in the model (4). Such a sharp difference of behavior cannot be appreciated when the active control is present, because the piezoelectric actuators determine a more exact control action, as earlier discussed. In this sense we can affirm that the presence of these actuators furnishes a certain degree of robustness to the control scheme.

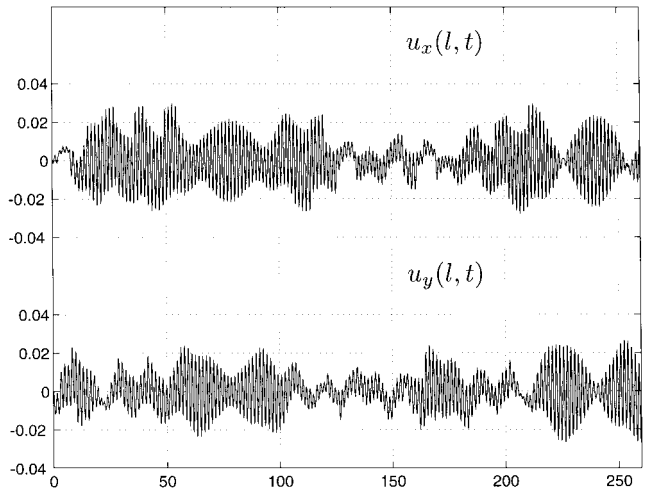

Fig. 10 Tip displacements $u_x(l,t)$ and $u_y(l,t)$, meters.

V. Conclusions

We have proposed dynamic controllers based only on spacecraft position and velocity measures. It is shown that active actuators, consisting of piezoelectric films bonded to the flexible appendages, can be successfully used not only for damping out small vibrations at the end of a slewing maneuver, but also when we deal with trajectory tracking in presence of input saturation. It results that such actuators increase the robustness of the controller. This suggests that robustness of control schemes can be obtained by exploiting structures containing a certain degree of actuation. Therefore, further research should address problems concerning structural parameter uncertainties.

Appendix: Spacecraft Parameters

Spacecraft:

$$J_0 = \begin{pmatrix} 414.27 & 2.7879 & 9.2362 \\ 2.7879 & 314.50 & 11.542 \\ 9.2362 & 11.542 & 210.73 \end{pmatrix}, \qquad J_r = \begin{pmatrix} 10 & 0 & 0 \\ 0 & 10 & 0 \\ 0 & 0 & 10 \end{pmatrix}$$

$$\delta_0 = \begin{pmatrix} 6.4182 & 3.5926 & -1.0837 \\ -22.2907 & -4.0724 & 0.8487 \\ -4.4891 & 6.4182 & 1.8061 \\ 4.0088 & -22.2907 & -1.4145 \\ 0 & 0 & 134.6129 \\ 0 & 0 & -129.3626 \end{pmatrix}$$

$$\delta_2 = \begin{pmatrix} 8.8003 \times 10^{-6} & 0 \\ -8.7996 \times 10^{-6} & 0 \\ 0 & 8.8003 \times 10^{-6} \\ 0 & -8.7996 \times 10^{-6} \\ 0 & 0 \\ 0 & 0 \end{pmatrix}$$

Flexible appendage (aluminum):

$$E_b = 6.8 \times 10^{10}\ \text{N/m}^2, \qquad t_b = 10^{-2}\ \text{m}, \qquad l = 1.5\ \text{m}$$

$$\omega_{x1} = \omega_{y1} = 22.6\ \text{rad/s}, \qquad \omega_{x2} = \omega_{y2} = 141.3$$

$$\omega_{z1} = 800.3, \qquad \omega_{z2} = 2328.6$$

$$\zeta_{x1} = \zeta_{y1} = \zeta_{z1} = 0.001, \qquad \zeta_{x2} = \zeta_{y2} = \zeta_{z2} = 0.00001$$

Bounding layer (Isotac):

$$E_{\text{bl}} = 1.1 \times 10^{6}\ \text{N/m}^2, \qquad t_{\text{bl}} = 0.42 \times 10^{-3}\ \text{m}$$

Piezoelectric layer (vinylidene fluoride):

$$E_p = 2 \times 10^9 \text{ N/m}^2, \qquad t_p = 2.1 \times 10^{-3} \text{ m}$$

$$d_p = 22 \times 10^{-12} \text{ m/V}$$

Acknowledgments

This research was supported by the Ministero dell'Università e della Ricerca Scientifica e Tecnologica, National Program Teoria dei Sistemi e del Controllo, and by the Agenzia Spaziale Italiana under Contract 94 RS 17. The author would like to thank Salvatore Monaco for the suggested research topic and Stefano Battilotti for his valuable comments. The author also thanks the anonymous referees for the helpful suggestions that led to improvements in the presentation of the results.

References

[1]Azam, M., Singh, S. N., Iyer, A., and Kakad, Y. P., "Detumbling and Reorientation Maneuvers and Stabilization of NASA SCOLE System," *IEEE Transactions on Aerospace and Electronic Systems*, Vol. 28, No. 1, 1992, pp. 80–91.

[2]Azam, M., Singh, S. N., Iyer, A., and Kakad, Y. P., "Nonlinear Rotational Maneuver and Vibration Damping of NASA SCOLE System," *Acta Astronautica*, Vol. 32, No. 3, 1994, pp. 211–220.

[3]Bach, R. E., and Paielli, R., "Linearization of Attitude-Control Error Dynamics," *IEEE Transactions on Automatic Control*, Vol. 38, No. 10, 1993, pp. 1521–1525.

[4]Biswas, S. K., and Ahmed, N. U., "Stabilization of a Class of Hybrid Systems Arising in Flexible Spacecraft," *Journal of Optimization Theory and Applications*, Vol. 50, No. 1, 1986, pp. 83–108.

[5]Dwyer, T. A. W., "Exact Nonlinear Control of Large Angle Rotational Maneuvers," *IEEE Transactions on Automatic Control*, Vol. 29, No. 9, 1984, pp. 769–774.

[6]Dwyer, T. A. W., Sira-Ramirez, H., Monaco, S., and Stornelli, S., "Variable Structure Control of Globally Feedback-Decoupled Deformable Vehicle Maneuvers," *Proceedings of the 26th IEEE Conference on Decision and Control* (Los Angeles, CA), Inst. of Electrical and Electronics Engineers Service Center, Piscataway, NJ, 1987, pp. 1281–1287.

[7]Hablani, H. B., "Multiaxis Tracking and Attitude Control of Flexible Spacecraft with Reaction Jets," *Journal of Guidance, Control, and Dynamics*, Vol. 17, No. 4, 1994, pp. 831–839.

[8]Kakad, Y. P., "Slew Maneuvers of Spacecraft Control Laboratory Experiment (SCOLE)," NASA CR-190228, April 1992.

[9]Monaco, S., and Stornelli, S., "A Nonlinear Feedback Control Law for Attitude Control," *Algebraic and Geometric Methods in Nonlinear Control Theory*, edited by M. Hazewinkel and M. Fliess, Reidel, Dordrecht, The Netherlands, 1985, pp. 573–595; also Univ. of Rome "La Sapienza," TR DIS-12.84, Rome, Italy, Dec. 1984.

[10]Monaco, S., and Stornelli, S., "A Nonlinear Attitude Control Law for a Satellite with Flexible Appendages," *Proceedings of the 24th IEEE Conference on Decision and Control* (Ft. Lauderdale, FL), Inst. of Electrical and Electronics Engineers Service Center, Piscataway, NJ, 1985, pp. 1654–1659.

[11]Monaco, S., Normand-Cyrot, D., and Stornelli, S., "Sampled Nonlinear Control for Large Angle Maneuvers of Flexible Spacecraft," *Proceedings of the 2nd International Symposium on Spacecraft Flight Dynamics* (Darmstadt, Germany), European Space Agency, European Space Research and Technology Center, Noordwijk, The Netherlands, 1986, pp. 31–38 (ESA SP-255).

[12]Monaco, S., Normand-Cyrot, D., and Stornelli, S., "On the Linearizing Feedback in Nonlinear Sampled Data Control Schemes," *Proceedings of the 25th IEEE Conference on Decision and Control* (Athens, Greece), Inst. of Electrical and Electronics Engineers Service Center, Piscataway, NJ, 1986, pp. 2056–2060.

[13]Monaco, S., Normand-Cyrot, D., and Stornelli, S., "Multirate Three Axes Attitude Stabilization of Spacecraft," *Proceedings of the 28th IEEE Conference on Decision and Control* (Tampa, FL), Inst. of Electrical and Electronics Engineers Service Center, Piscataway, NJ, 1989, pp. 797–802.

[14]Singh, S. N., "Robust Nonlinear Attitude Control of Flexible Spacecraft," *IEEE Transactions on Aerospace and Electronic Systems*, Vol. 23, No. 3, 1987, pp. 380–387.

[15]Singh, S. N., "Rotational Maneuver of Nonlinear Uncertain Elastic Spacecraft," *IEEE Transactions on Aerospace and Electronic Systems*, Vol. 24, No. 2, 1988, pp. 114–123.

[16]Wen, J. T., and Kreutz-Delgado, K., "The Attitude Control Problem," *IEEE Transactions on Automatic Control*, Vol. 36, No. 10, 1991, pp. 1148–1162.

[17]Wie, B., and Barba, P. M., "Quaternion Feedback for Spacecraft Large Angle Maneuvers," *Journal of Guidance, Control, and Dynamics*, Vol. 8, No. 3, 1985, pp. 360–365.

[18]Annaswamy, A. M., and Clancy, D. J., "Adaptive Control Strategies for Flexible Space Structures," *IEEE Transactions on Aerospace and Electronic Systems*, Vol. 32, No. 3, 1996, pp. 952–965.

[19]Singh, S. N., "Nonlinear Adaptive Attitude Control of Spacecraft," *IEEE Transactions on Aerospace and Electronic Systems*, Vol. 23, No. 3, 1987, pp. 371–379.

[20]Georgiou, G., Di Gennaro, S., Monaco, S., and Normand-Cyrot, D., "On the Nonlinear Adaptive Control of a Flexible Spacecraft," *Proceedings of the 1st ESA Conference on Spacecraft Guidance, Navigation, and Control Systems* (Noordwijk, The Netherlands), European Space Agency, European Space Research and Technology Center, Noordwijk, The Netherlands, 1991, pp. 509–514 (ESA SP-323).

[21]Crawley, E. F., and de Luis, J., "Use of Piezoelectric Actuators as Elements of Intelligent Structures," *AIAA Journal*, Vol. 25, No. 10, 1987, pp. 1373–1385.

[22]Yang, S. M., and Lee, Y. J., "Modal Analysis of Stepped Beams with Piezoelectric Materials," *Journal of Sound and Vibration*, Vol. 176, No. 3, 1994, pp. 289–300.

[23]Baz, A., and Poh, S., "Performance of an Active Control System with Piezoelectric Actuators," *Journal of Sound and Vibration*, Vol. 126, No. 2, 1988, pp. 327–343.

[24]Burke, S. E., and Hubbard, J. E., Jr., "Distributed Actuator Control Design for Flexible Beams," *Automatica*, Vol. 24, No. 5, 1988, pp. 619–627.

[25]Li, Z., and Bainum, P. M., "Vibration Control of Flexible Spacecraft Integrating a Momentum Exchange Controller and a Distributed Piezoelectric Actuator," *Journal of Sound and Vibration*, Vol. 177, No. 4, 1994, pp. 539–553.

[26]Bailey, T., and Hubbard, J. E., Jr., "Distributed Piezoelectric-Polymer Active Vibration Control of a Cantilever Beam," *Journal of Guidance, Control, and Dynamics*, Vol. 8, No. 5, 1985, pp. 605–611.

[27]Hyland, D. C., Junkins, J. L., and Longman, R. W., "Active Control Technology for Large Space Structures," *Journal of Guidance, Control, and Dynamics*, Vol. 16, No. 5, 1993, pp. 801–821.

[28]Ickes, B. P., "A New Method for Performing Digital Control System Attitude Computations Using Quaternions," *AIAA Journal*, Vol. 8, No. 1, 1970, pp. 13–17.

[29]Yuan, J. S. C., "Closed-Loop Manipulator Control Using Quaternion Feedback," *IEEE Journal of Robotics and Automation*, Vol. 4, No. 4, 1988, pp. 434–440.

[30]Meirovitch, L., *Analytical Methods in Vibrations*, Macmillan, New York, 1967.

[31]Goldstein, H., *Classical Mechanics*, Addison–Wesley, Reading, MA, 1965.

[32]Sastry, S. S., and Bodson, M., *Adaptive Control: Stability, Convergence, and Robustness*, Prentice–Hall, Englewood Cliffs, NJ, 1989.

[33]Khalil, H. K., *Nonlinear Systems*, Macmillan, New York, 1992.

[34]Curtain, R. F., and Pritchard, A. J., *Functional Analysis in Modern Applied Mathematics*, Academic, New York, 1977.